THE EFFECTS OF OUT-OF-PLANE CURVATURE ON UNIFORMLY SHEARED TURBULENCE

Dale C. Roach*
A. Gordon L. Holloway
Department of Mechanical Engineering
University of New Brunswick
PO Box 4400
Fredericton, N.B.
E3B 5A3
Canada
holloway@unb.ca
droach@unbsj.ca

ABSTRACT

This paper describes recent experiments conducted at the University of New Brunswick in which uniformly sheared turbulence was subjected to plane mean flow curvature not coincident with the plane of the shear. One of the results was a swirling mean motion that caused the uniform shear to rotate about the tunnel centerline. In the first portion of the flow, the swirl was weak and the turbulence was subjected to plane curvature perpendicular to the plane of the shear. In the second portion, the swirl was well developed and the mean shear had been rotated by 30° towards the plane of the curvature. Measurements of all components of the mean velocity, Reynolds stress, and streamwise integral length scales are reported.

1 - INTRODUCTION

Flow curvature has been shown to play an important role in determining the structure of turbulent shear flows that occur with pumps, turbines, airplanes and automobiles. These flow curvatures are often complex and have a three-dimensional form. However, most studies of curvature have been concerned with the two-dimensional streamwise curvature, where the shear and curvature lie in the same plane. These flows are relatively simple to construct in the laboratory and have important practical applications. Measurement of these flows has shown that sheared turbulence is very sensitive to streamwise curvature; stabilizing it when the shear is directed away from the center of curvature, and destabilizing it when the shear is directed towards the center of curvature. The present experiment addresses the problem of three-dimensional curvature, albeit in a simple form. It examines the effects of subjecting a uniform turbulent shear flow to plane curvature that is initially perpendicular to the plane of the mean shear. A schematic of this arrangement is depicted in Figure 1 where the mean velocity profile shown corresponds to that at the entrance of the curved wind tunnel and the s coordinate corresponds to the wind tunnel centerline. The development of this shear flow is strongly affected by the streamwise component of mean vorticity that develops as a result of the curvature. This swirling motion rotates the mean shear about the streamwise direction so that the flow tends to a case of two-dimensional streamwise curvature. In the present experiment the shear is rotated towards the positive n direction by up to 30° and the turbulence growth rate is diminished.

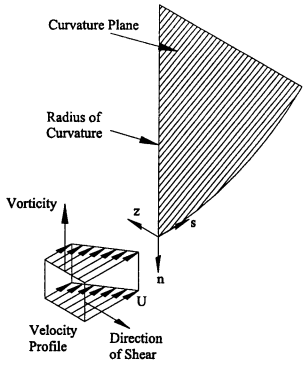

Figure 1: A curved uniform shear flow where the shear and curvature lie in different planes. The shear shown coincides with the mean conditions at the entrance of the curved tunnel. The velocity components in the s, n ,z directions are u,v,w.

2 - APPARATUS

The experimental facility used in this study was an open-return wind-tunnel with a shear generator, a 5 m X 0.55 m X 0.55 m straight section, and a curved test section which turned the flow by 60° (Roach 2001). The straight section allowed for the development of the sheared turbulence to a self-preserving state (Karnik and Tavoularis, 1987) before it was guided tangentially into the curved

* Present address: Department of Engineering, University of New Brunswick, P.O. Box 5050, Saint John, N.B., E2L 4L5

tunnel. The flow had a centerline speed of approximately 9.5 m/s, a shear rate of 21 s^{-1} and a centerline radius of 3 m. The corners of the curved tunnel were filleted and some suction was applied to the low speed side to aid in the maintenance of the flow. Measurements were performed using standard hot-wire anemometry and a computer controlled positioning system. Velocity data was acquired at 4 cm intervals along the centerline of the tunnel and at nine planes perpendicular to the streamwise direction in the curved section. The integral lengthscales were calculated from temporal autocorrelations using Taylor's frozen flow hypothesis and integration to the first zero crossing. From the measurements conducted it was found that the turbulence was approximately homogeneous within the core of the tunnel over planes perpendicular to the streamwise direction. The development of turbulence structure under the influence of curvature was revealed by measurements taken along the tunnel centerline.

3 - MEAN FLOW

For the configuration shown in Figure 1, the shear flow at the start of the curved tunnel will develop into a swirling curved shear flow. The mechanism through which this occurs is described in detail by the analysis of Roach and Holloway (2000) and Roach (2001). The results of their inviscid analysis show that the components of the vorticity for this flow, expressed in the curvilinear coordinate system of figure 1, are given by

$$\zeta_n = \left|\vec{\zeta}_{nz,o}\right| \sin(\alpha) \qquad (1)$$

$$\zeta_z = \left|\vec{\zeta}_{nz,o}\right| \cos(\alpha) \qquad (2)$$

$$\frac{d\zeta_s}{ds} = -\frac{2\left|\vec{\zeta}_{nz,o}\right| \sin(\alpha)}{R_c} \qquad (3)$$

where α is the angle between the projection of the vorticity vector on the n-z plane and the n direction. It can be calculated from

$$\frac{d\alpha}{ds} = \frac{\zeta_s}{2U} \qquad (4)$$

Equations (1) and (2) reveal that the projection of the vorticity vector on the n-z plane remains constant since

$$\zeta_n^{\,2} + \zeta_z^{\,2} = \left|\vec{\zeta}_{nz,o}\right| \qquad (5)$$

This implies that the swirling flow remains a shear flow if viewed in the correct rotating frame.

The measured streamwise development of the mean vorticity components is shown in Figure 2. The vorticity is in the negative n direction when the flow enters the curved tunnel because the shear is in the (s,z) plane. As predicted by equations (1)-(4), the imposition of curvature generates ζ_s which, in turn, causes rotation of the total vorticity vector about the streamwise axis. Furthermore, as ζ_z increases in magnitude, ζ_n begins to fall in such a way that (5) is nearly satisfied.

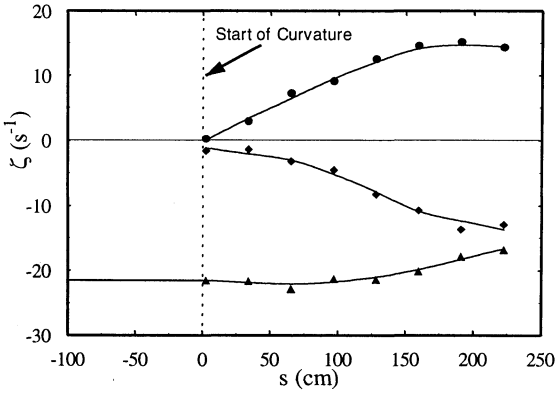

Figure 2: Streamwise development of the vorticity (ζ_s:●, ζ_n:▲, ζ_z:◆). Solid lines are fit through the data. The sum $\zeta_n^{\,2} + \zeta_z^{\,2} \cong$ constant.

Figure 3 shows contours of the streamwise mean velocity and projections of the mean velocity vector on the n-z plane for measurement station 8. It is clear that a swirling motion has developed and that the gradient of mean velocity has been rotated by approximately 30° about the streamwise axis of the tunnel.

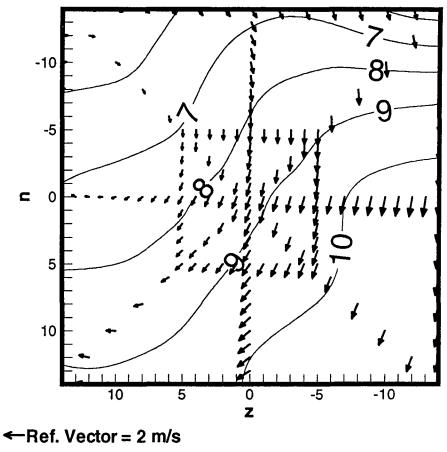

Figures 3: Mean flow at station 8. Speed contours are in m/s. The flow region shown includes only the central core of the tunnel (in cm) and excludes the tunnel boundary layers.

4 – TURBULENCE

4.1 - Effects on the Kinetic Energy and Length Scales

The measured streamwise development of twice the turbulence kinetic energy per unit mass, defined as

$$\overline{q^2} = \overline{u^2} + \overline{v^2} + \overline{w^2} \qquad (6)$$

is shown in Figure 4. Near the end of the straight section this quantity can be seen to grow nearly exponentially as described by Karnik and Tavoularis (1987). From the point where the curvature was applied, the rate of growth is decreased until $\overline{q^2}$ reached a maximum at s = 175 cm and then decreased for s > 225 cm.

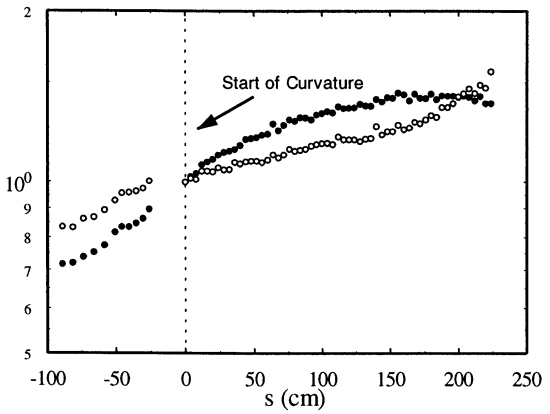

Figure 4: Streamwise development of $\overline{q^2}$ (●) and L(○) (Normalized with the respective value at s = 0)

The reduction of kinetic energy growth rate in this flow, despite the presence of the mean shear, suggests the curvature has a stabilizing effect. An explanation of this behavior based on the production of turbulence is provided in the discussion.

In order to determine the effects of the curvature on the streamwise integral lengthscales, an average lengthscale, which is invariant to rotation, can be calculated similar to $\overline{q^2}$. It is given by

$$L = \frac{\overline{u^2}}{\overline{q^2}} L_{uu} + \frac{\overline{v^2}}{\overline{q^2}} L_{vv} + \frac{\overline{w^2}}{\overline{q^2}} L_{ww} \qquad (7)$$

The measured streamwise development of this quantity is shown in Figure 4. Near the end of the straight section L grows nearly exponentially and continues to grow with nearly the same slope through most of the curved tunnel. After s=150 cm the rate of growth of L increases, contrary to the measured behavior $\overline{q^2}$. It seems that the turbulence is losing energy but increasing in scale.

4.2 – Effects on the Reynolds Stresses

The degree to which the structure of the turbulence is affected by curvature was evaluated using the Reynolds stress anisotropy tensor defined as

$$\mathbf{m} = \begin{pmatrix} \frac{\overline{u^2}}{\overline{q^2}} - \frac{1}{3} & \frac{\overline{uv}}{\overline{q^2}} & \frac{\overline{uw}}{\overline{q^2}} \\ \frac{\overline{uv}}{\overline{q^2}} & \frac{\overline{v^2}}{\overline{q^2}} - \frac{1}{3} & \frac{\overline{vw}}{\overline{q^2}} \\ \frac{\overline{uw}}{\overline{q^2}} & \frac{\overline{vw}}{\overline{q^2}} & \frac{\overline{w^2}}{\overline{q^2}} - \frac{1}{3} \end{pmatrix} \qquad (8)$$

Near the end of the straight tunnel section, before the application of curvature, m has the values

$$\mathbf{m} = \begin{pmatrix} 0.25 & 0.00 & 0.13 \\ 0.00 & -0.08 & 0.00 \\ 0.13 & 0.00 & -0.17 \end{pmatrix} \qquad (9)$$

Equation (9) is slightly more anisotropic than those measured by Holloway and Tavoularis, (1992) for uncurved, uniform shear flow.

The streamwise development of the components of the stress anisotropy tensor are shown in Figure 5.

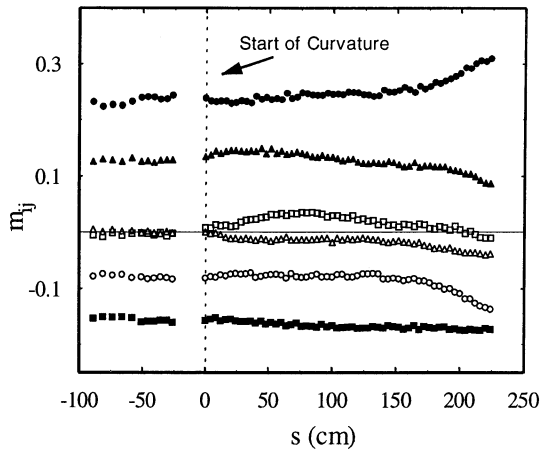

Figure 5: Streamwise development of the dimensionless turbulence stress anisotropy (m_{uu}:●, m_{vv}:○, m_{ww}:■, m_{uv}:□, m_{uw}:▲, m_{vw}:Δ)

Prior to s = 150 cm, m_{uu} gradually increases, m_{ww} decreases, and m_{vv} remains nearly constant. (Note

that by definition $m_{uu} + m_{vv} + m_{ww} = 0$) As the strength of the swirl increases towards the end of the tunnel, m_{vv} begins to fall more quickly which is balanced by a rise in m_{uu} while m_{ww} remains unaffected.

For the shear stresses, m_{uv} shows a gradual increase immediately after the imposition of curvature. This trend is then reversed, however, as the swirling motion begins to develop. The dominant turbulence shear stress, m_{uw}, decreases slowly and steadily for the first two-thirds of the curved tunnel. Once the streamwise vorticity increases and the shear begins to rotate more rapidly the change accelerates. The third turbulence shear stress, m_{vw}, also shows a slight decrease at the entrance to the curved section. Then, as the streamwise vorticity increases, the changes to m_{vw} become more pronounced and it becomes increasingly negative. Further explanation for the development of the shear stresses will be covered in the discussion.

The coordinate system used to describe the results remains tangent to the centreline of the tunnel as it moves along the curve but does not rotate with the mean shear. To detemine the extent to which the choice of coordinates influences the changes in the anisotropy the second invariant of the anisotropy tensor, *II*, as given by Lumley and Newman (1977) has been considered

$$II = m_{uu}^2 + m_{vv}^2 + m_{ww}^2 + 2m_{uv}^2 + 2m_{uw}^2 + 2m_{vw}^2 \quad (10)$$

The streamwise variation of *II* can be seen in Figure 6.

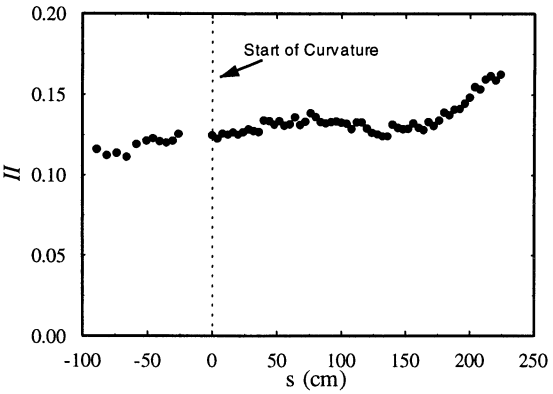

Figure 6: Streamwise development of the second invariant of the Reynolds stress anisotropy tensor.

This figure shows that the stress anisotropy increases gradually over the first two-thirds of the curved section of the tunnel. In the last third of the tunnel, the anisotropy experiences increases more rapidly.

4.3 – Effects on the Integral Lengthscales

To investigate the behavior of the streamwise integral lengthscales, techniques similar to those used for the analysis of the turbulence stresses will be employed. The lengthscale anisotropy tensor is defined as

$$\mathbf{n} = \begin{pmatrix} 0 & \frac{L_{uv}}{L} & \frac{L_{uw}}{L} \\ \frac{L_{vu}}{L} & \frac{L_{vv} - L_{uu}/2}{L} & \frac{L_{vw}}{L} \\ \frac{L_{wu}}{L} & \frac{L_{wv}}{L} & \frac{L_{ww} - L_{uu}/2}{L} \end{pmatrix} \quad (11)$$

Near the end of the straight tunnel section, before the start of curvature, **n** was measured to be **n** is

$$\mathbf{n} = \begin{pmatrix} 0 & 0 & 1.12 \\ 0 & -0.04 & 0 \\ 1.12 & 0 & -0.13 \end{pmatrix} \quad (12)$$

Here only n_{vv}, n_{ww}, n_{uv}, n_{uw} and n_{vw} have been computed. The development of these five components of the tensor can be seen in Figure 7. Note that because the magnitudes of $\overline{uv}$ and $\overline{vw}$ are small and in some cases they change sign, large errors in n_{uv} and n_{vw} can result. Where this is the case, the data has been removed from the figure.

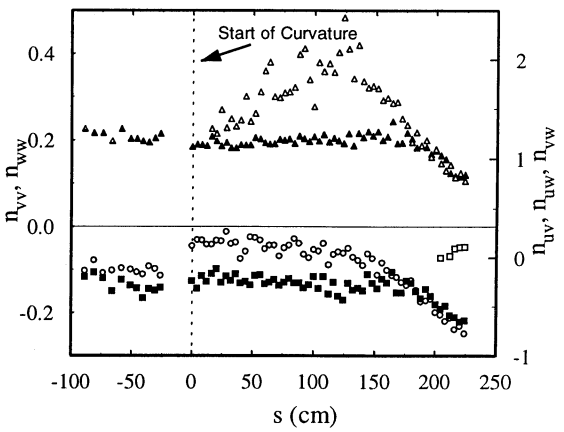

Figure 7: Streamwise development of the dimensionless integral lengthscale anisotropy (n_{vv}:○, n_{ww}:■, n_{uv}:□, n_{uw}:▲, n_{vw}:Δ)

Figure 7 shows that as the flow develops, the n_{vv} and n_{ww} components are initially unaffected by the application of out-of-plane curvature. The n_{vv} component does eventually begin to decrease and crosses the n_{ww} data , which is also decreasing.

At the entrance to the curved section, n_{uw} is 1.12 and remains relatively constant for the first two thirds of

the curved section. As the rotation of the shear becomes more significant, n_{uw} begins to decrease. Comparing Figure 7 with Figure 5, it is found that the points where m_{uw} and n_{uw} begin to fall nearly coincide.

DISCUSSION

The production of the turbulence kinetic energy in a swirling curved shear flow can be reduced to

$$P_{\frac{q^2}{2}} = 2\vec{\sigma}_\tau \cdot \vec{d}_\tau \qquad (13)$$

where

$$\vec{\sigma}_\tau = 0\vec{e}_s - \overline{uv}\vec{e}_n - \overline{uw}\vec{e}_z \qquad (14)$$

and

$$\vec{d}_\tau = 0\vec{e}_s + \left(\frac{\partial U}{\partial n} - \frac{U}{R_c}\right)\vec{e}_n + \frac{\partial U}{\partial z}\vec{e}_z \qquad (15)$$

From equation (12) it can be seen that the production due to shear will be maximized when the turbulence stress $\vec{\sigma}_\tau$ and the shear strain-rate $\vec{d}_\tau$ vectors are perfectly aligned. To examine the variation of the angle between these two vectors, the stress and strain-rate unit vectors at each of the measurement planes in the tunnel have been shown in Figure 8.

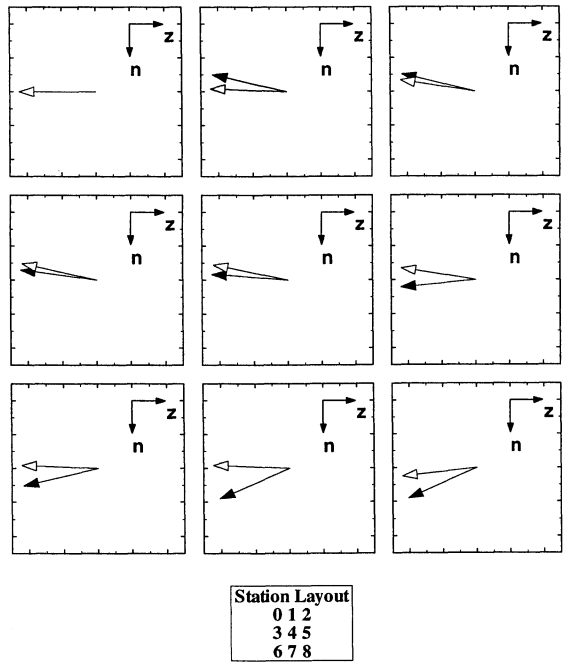

Figure 8: Mean shear strain-rate (solid) and turbulence shaer stress (hollow) unit vectors shown at different stations in the windtunnel.

CONCLUSION

Initially, the turbulence stress and shear strain-rate vectors are aligned as is the case for rectilinear shear flow. When curvature is applied, the shear strain-rate vector tilts upward due to the extra strain (see equation 15). The shear strain-rate vector then remains relatively unaffected up to station 4 where the swirl has developed sufficiently to cause it to rotate about the streamwise axis. This rotation continues throughout the remainder of the tunnel. The trend for the development of turbulence shear stress follows that of the shear strain-rate vector very closely with the notable exception that $\vec{\sigma}_\tau$ lags the development of the shear strain-rate vector. This lag causes a decrease in the production. Not evident in the figure is the fact that the magnitude of the turbulence shear stress vector is decreasing which causes a further decrease in the production.

The flow exhibited two distinct regions of behavior. In the first of these, which existed from s = 0 up to approximately s = 100 cm, the flow was mainly subjected to out-of-plane curvature without appreciable swirl. In this region it was found that there was little response from the anisotropy of the turbulence stresses and integral lengthscales though there was some mild development of the out-of-plane components of the stress and integral lengthscale anisotropies. The growth rate of the energy was diminished in this region below the value found in the straight section of the tunnel. In the second region, the swirl was well developed and caused significant rotation of the mean shear. The growth rate of $\overline{q^2}$ was reduced to zero and rate of growth L was increased. Furthermore, the dimensionless stress and lengthscale anisotropies showed much more rapid variation than in the first part of the tunnel though the observed effects lagged the development of the mean shear. It would seem the out of plane curvature without swirl has a relatively weak effect on the turbulence structure.

References

Karnik, U. and Tavoularis, S., 1989 "Further experiments on the evolution of turbulent stresses and scales in uniformly sheared turbulence", Journal of Fluid Mechanics, Vol. 204, pp. 457-478.

Roach, D.C. and Holloway, A.G.L., 2000 "The Generation of Swirl in Curved Shear Flow", CSME Forum 2000, Montréal, Canada, May 19-23

Roach, D.C., 2001, Ph.D. Thesis, Department of Mechanical Engineering, University of New Brunswick, Fredericton, New Brunswick, Canada.

Holloway, A.G.L. and Tavoularis, S., 1992 "The effects of curvature on sheared turbulence", Journal of Fluid Mechanics, Vol. 237, pp. 569-603

Lumley, J.L. and Newman, G.R., 1977 "The return to isotropy of homogeneous turbulence", Journal of Fluid Mechanics, Vol. 82, pp. 161-178